Analysis and Rapid Calculation of Magnetic Thermal Coupling Characteristics of Large Power Transformers

Hong Liu[1,*], Guodong Li[1], Xuan Wang[1], Hua Yu[1],·Bin Li[2], Tong Song[2], Changjiang Na[2], Haibo Wang[2]
[1]State Grid Shanxi Electric Power Company Electric Power Science Research Institute,
030001 Tai Yuan, China
[2]Baoding Tianwei Xinyu Technology Development Co., Ltd,
071051 Bao Ding, China
[*]512048680@qq.com; liuhong_19870409@163.com; 519967925@qq.com;yuhua16885@163.com; 278555787@qq.com; songtong0707@126.com; nann321@126.com; 316620314@qq.com

***Abstract*—Conventional single-phase nuclear main transformers are susceptible to certain risks such as an increase in high local temperature in the windings, high leakage fields, and high short-circuit forces. Moreover, these transformers are too costly to use. In this paper, simulation and test studies are carried out for a 500 kV single-phase two-core column nuclear power main transformer. First, using the principle of fluid-thermal coupling simulation, a three-dimensional simulation of a single-phase two-core column nuclear power main transformer is performed to obtain its temperature field distribution, and the accuracy of the established 3D model is validated through experimental tests. Second, because the 3D simulation calculation time is long, the computer occupies a large amount of memory, but the 3D winding temperature distribution in the allowable error range in line with the axisymmetric distribution can be replaced by the 2D axisymmetric model. Therefore, a two-dimensional axisymmetric simulation is conducted for a single-phase two-core column nuclear power main transformer. Simultaneously, the h-type adaptive mesh refinement method is used to optimise the two-dimensional mesh distribution based on the coupled fluid-thermal field. The optimised simulation results are compared with those from the three-dimensional model and experimental tests, confirming the accuracy of the two-dimensional approach. Finally, the winding temperature distribution under various loading conditions is computed via a two-dimensional optimised simulation and validated against the three-dimensional temperature profile, thereby verifying the precision of the two-dimensional method. The temperature data obtained under different operational loads can serve as a critical dataset to construct a digital twin model of the transformer.**

***Index Terms*—Transformer cores; Magnetic losses; Finite element analysis; Power transformers.**

I. INTRODUCTION

Multiphysical field transformer numerical computations, which are the virtual layer of the digital twin technology architecture of the transformer, are important for digital transformations [1], [2]. It is essential to obtain an accurate internal temperature field distribution of the transformer, as this analysis provides instructive guidance for structural optimisation [3], [4]. The rise in internal temperature of a transformer serves as a critical indicator of its thermal performance. Excess temperature elevation accelerates thermal degradation of insulation materials, leading to compromised dielectric strength, reduced operational lifespan, and ultimately jeopardising the safety and stability of power transformer operation. This correlation is often quantified by the Montsinger rule, where a sustained temperature increase of 6 °C–10 °C can potentially halve the insulation life [5]–[8]. Therefore, it is critical to accurately calculate the temperature rise distribution of the internal components of the transformer and to use it as the basis for transformer design. A single-phase nuclear power main transformer constitutes a critical component within the power grid infrastructure and plays a vital role in the efficient and reliable transmission and distribution of electrical energy generated by nuclear power plants. Due to its large capacity, it leads to a longer iron core and windings, and the transformer overall occupies more space and incurs higher costs. To address these problems, a single-phase two-core transformer can be very good at reducing space requirements and cost. Under the same capacity, the height of a single-phase two-core transformer is 1/2 of the height of an ordinary single-phase transformer. Due to its special two-core column structure, it can also greatly reduce the risk of a high local temperature rise in windings, leakage fields [9], [10], short-circuit forces, etc. [11], [12]. Consequently, the precise determination of winding temperature rise is fundamental to the design and operation of single-phase two-core column nuclear power main transformers, as it forms the basis for effective thermal management and operational safety.

In terms of fluid-thermal coupling analysis of power equipment, an increasing number of studies have been conducted to combine digital twin technology with fluid-thermal coupling field calculations [13]. For example, for a single-phase double-winding transformer with the help of digital twin technology to establish a high-fidelity simulation model with the transformer entity with the same structure,

Manuscript received 11 May, 2025; accepted 29 July, 2025.
This research was supported by the Science and Technology Project of State Grid Shanxi Electric Power Company under Grant No. 520530250013.

size, and material physical property parameters of the transformer, a high-fidelity simulation model of the transformer is developed to study the impact of turn-to-turn faults on the electrical and thermal characteristics of the parameter. For a three-phase, three-column transformer, the structural parameters of the physical equipment and the real-time electrical quantities are used to establish the state-space model under different operating conditions. The digital twin model is corrected through the actual data, the virtual world and the physical world are synchronised, and the discrete iterative method and Z-transform method are used to solve the model comprehensively to improve the sensitivity of fault identifications. Combined with computational fluid dynamics theory and a genetic algorithm, the winding structure of a dry-type transformer was optimised [14]. The heat dissipation structure of the three-phase transformer is optimised by the response surface method [15]. The optimal structural parameters of the transformer windings were obtained by orthogonal testing and range and variance analysis [16]. The results show that the temperature field of the single-phase two-core column nuclear power main transformer is less studied, and the digital mirror model obtained by 3D simulation is computationally intensive and has poor real-time performance.

Based on the above problems, the 2D axisymmetric modelling of a 500 kV single-phase two-core column nuclear power main transformer is performed in this study, and the results of the temperature field calculation are compared with the 3D model and test data. The calculation speed of the model is greatly improved while the accuracy is maintained. Moreover, a solution is provided for the real-time calculation of digital twin transformers [17]. First, the 3D simulation calculation of a single-phase two-core column nuclear power main transformer is carried out based on the principle of fluid-thermal coupling simulation, the 3D temperature field distribution is obtained, and the accuracy of the 3D simulation model is verified through tests. Second, because the 3D simulation calculation time is long, the computer occupies a large amount of memory, but the 3D winding temperature distribution in the allowable error range in line with the axisymmetric distribution can be replaced by the 2D axisymmetric model. Therefore, a 2D axisymmetric simulation of a single-phase two-core column-type nuclear power main transformer is carried out, and at the same time, the h-type adaptive mesh control method is adopted to optimise the 2D mesh through the distribution of the fluid-thermal coupling field. The optimisation simulation results obtained are compared with the 3D simulation results and the test results, and the accuracy of the 2D optimisation simulation results is verified [18]. Finally, the winding temperature distribution under different loading conditions is calculated by a 2D optimisation simulation and compared with the 3D winding temperature distribution to verify the accuracy of the 2D simulation. Temperature data under different loading conditions can provide a data basis for the establishment of digital twin modelling of single-phase two-core column-type nuclear power main transformers.

II. BASIC STRUCTURE OF A SINGLE-PHASE TWO-CORE COLUMN NUCLEAR POWER MAIN TRANSFORMER

The physical diagram and structural diagram of the 500 kV single-phase two-core column forced oil circulating air-cooled transformer body are shown in Fig. 1. Its body structure mainly includes windings, iron cores, pull plates, and clamps. The structure of the iron core is a two-core column type, so the purpose of the design is to save space and cost. The transformer winding is divided into high-voltage and low-voltage parts, of which the low-voltage winding is divided into two layers to better dissipate heat. The arrangement of transformer windings and the winding connection principle are shown in Fig. 2. The high-voltage winding in the A-column is wound from both ends of the winding, the winding direction of the upper part is to the right, and the winding direction of the lower half is to the left. The high-voltage winding within the X-column is configured to be wound from both of its ends, exhibiting a winding direction that is reversed relative to that of the winding in the A-column. Finally, the wires in the two columns are led out from the middle. The low-voltage winding in the A-column is wound from the outer upper part of the winding. The low-voltage winding in the A-column is wound from the outer upper end to the bottom, connecting the bottom of the inner low-voltage winding and the winding to the upper end, and the winding method of the X-column is the same as that of the A-column.

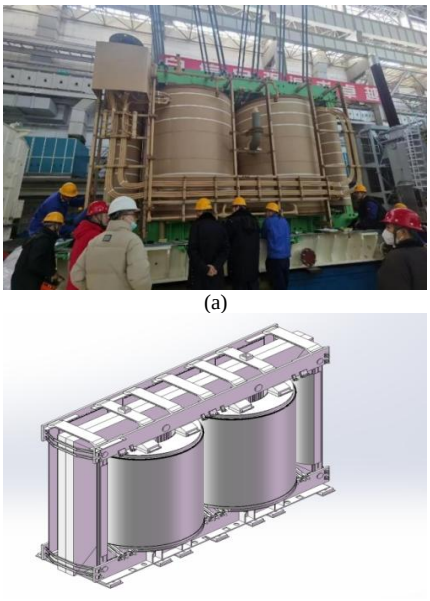

(a)

(b)

Fig. 1. Physical and structural drawings of the transformer body: (a) Physical drawing of the body; (b) Structure of the body.

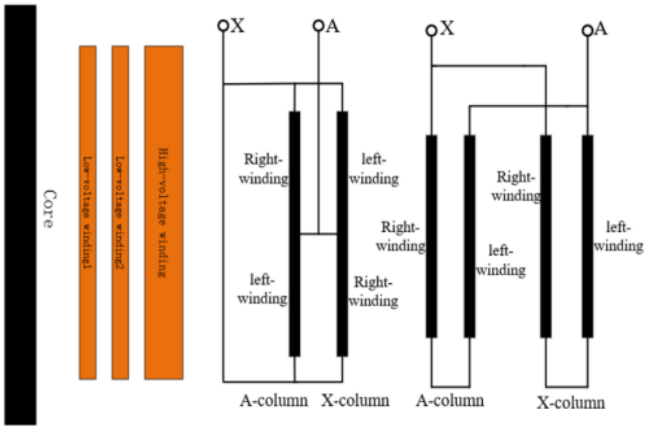

Fig. 2. Transformer winding arrangement and winding connections.

III. 3D TRANSFORMER SIMULATION AND ANALYSIS

A. Coupled Fluid-Thermal Control Equations

The temperature field calculation of a single-phase two-core nuclear power main transformer includes two parts: the winding temperature rise heat conduction and the oil flow heat transfer. The transformer oil in the oil passage is forced convection and the oil flow rate is low, corresponding to a small Reynolds number. Thus, it is regarded as laminar flow. According to the Navier-Stokes equation, the control equation for the calculation of the transformer fluid-thermal coupling is [19]:

$$\frac{\partial \rho}{\partial t} + \nabla \times (\rho v) = 0, \tag{1}$$

$$\rho \frac{\partial v}{\partial t} + \rho v \times \nabla v = -\nabla p + \nabla \tau + F + \rho g, \tag{2}$$

$$\rho c_p \frac{\partial T}{\partial t} + \rho c_p v \times \nabla T = \nabla \times (k_t \nabla T) - p \nabla \times v + \tau : \nabla v + Q, \tag{3}$$

where ρ denotes the fluid density, v represents the velocity vector, p designates the fluid pressure, τ is the viscous stress tensor, F accounts for external forces, g indicates the gravitational acceleration, c_p refers to the constant-pressure specific heat capacity, T stands for the temperature, k_t denotes the thermal conductivity, Q represents the heat source term, and ∇ is the Hamiltonian operator.

B. 3D Simulation Model of a Single-Phase Two-Core Column Transformer

According to the physical construction of the transformer, its 3D simulation geometry model is shown in Fig. 3. The transformer is a single-phase two-core column type, and its main structure includes an iron core, pull plate, clamp, winding, transformer oil, shell, and other structures. The size of the transformer shell is 3.2 m × 6.5 m × 4.255 m, and the modelling can be ignored to pull the tape, pads, and screws and other components that have a small impact on the temperature distribution, thus reducing the number of meshes and computational workload.

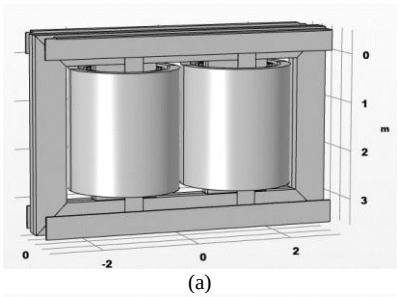

(a)

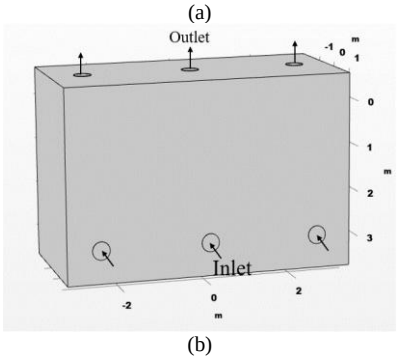

(b)

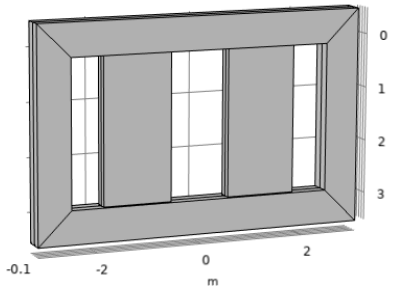

(c)

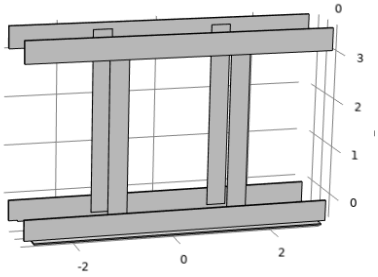

(d)

Fig. 3. Structure of the 3D simulation model of the transformer: (a) Transformer body; (b) Shell; (c) Core; (d) Pulling plates, Clamps.

C. Parameter Setting

During coupled fluid-thermal field simulation of oil-immersed transformers, convective circulation of the insulating oil serves as the dominant mechanism for transferring heat away from the energised core and windings. In computational studies focussing on predicting the temperature rise characteristics of transformers, the physical parameters of the insulating oil are frequently treated as invariable constants to simplify the thermal modelling process. Key thermophysical properties of transformer oil, including its constant-pressure heat capacity, thermal conductivity, dynamic viscosity, and density, exhibit significant temperature dependence under real-world operating conditions. Therefore, to more accurately simulate the thermal behaviour of oil-immersed transformers and enhance result fidelity, the thermophysical properties of the transformer oil are defined as temperature-dependent functions, as detailed in Table I.

TABLE I. PHYSICAL PARAMETERS OF TRANSFORMER OIL.

Physical parameters	Transformer oils
Constant-pressure heat capacity (J/(kg × k))	$-0.001522T^2 + 5.191T + 455.9$
Densities (kg/m^3)	$0.0003612T^2 - 0.826T + 1093$
Thermal conductivity (W/(m × K))	$1.434\times10^{-20}T^2 - 7.647\times10^{-5}T + 0.1538$
Viscosity of dynamics (Pa × s)	$2.055\times10^{-6}T^2 - 0.001533T + 0.2886$

In addition to the oil of the transformer, heat conduction inside the core, winding, pull plate, clamp, etc., will also affect the temperature rise of the transformer. Since temperature has a weak influence on its physical parameters, it is set as a constant in this paper, and the specific parameters are shown in Table II.

The dissipation of thermal energy from the core and windings, resulting from electromagnetic losses, constitutes a fundamental phenomenon during the operation of oil-

immersed transformers.

TABLE II. PHYSICAL PARAMETERS OF THE WINDING OF THE CORE PULLING PLATE CLAMPING PIECE.

Physical parameters	Core	Pulling plates, Clamps	Windings
Constant-pressure heat capacity J/(kg × k))	501.8	480	385
Constant-pressure heat capacity J/(kg × k))	21	48	400
Densities (kg/m³)	7650	7800	8960

In this paper, the temperature rise characteristics are mainly analysed. According to the results of the electromagnetic loss calculation, the energy generated by it is given in the form of a heat dissipation rate. The heat dissipation rate is as follows: 120800 W in the iron core, 230260 W in the low-voltage winding, 520000 W in the high-voltage winding, 27332 W in the pull plate, and 12626 W in the clamping. For the three-dimensional steady-state simulation of the oil-immersed transformer's coupled fluid-flow and heat transfer, key operational boundary conditions were imposed: an ambient temperature of 26 °C was set, with transformer oil entering through a shell-side inlet at a velocity of 2.12 m/s.

D. 3D Simulation Results and Analysis

Under a rated load condition with an ambient temperature of 26 °C, the temperature distributions of the high-voltage (HV) and low-voltage (LV) windings of the transformer are illustrated in Fig. 4. The results indicate that the hot spot temperature is predominantly located in the upper section of the windings, with the region adjacent to the core column exhibiting the highest values. Specifically, the maximum temperature of the HV winding reaches 49.9 °C, while that of the LV winding is 43.6 °C.

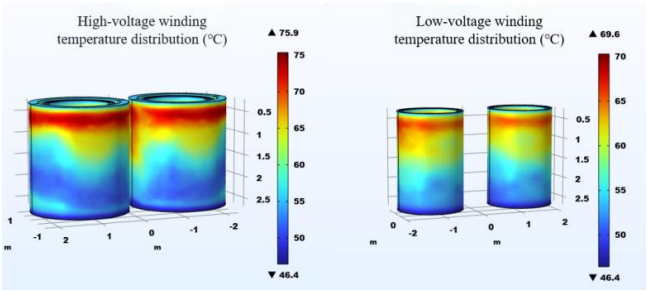

Fig. 4. Temperature distribution of the windings inside the transformer.

The cross-sectional temperature profile of the 5th disk (cake) of both the HV and LV windings is presented in Fig. 5, and its corresponding linear temperature distribution is shown in Fig. 6. Eight uniformly spaced points were selected along the cross-section of the 5th disk, encompassing both the maximum and minimum temperature values. As observed in Figs. 5 and 6, the 5th disk of the HV winding exhibits a maximum temperature of 49.9 °C and a minimum of 45.3 °C, while the 5th disk of the LV winding shows a maximum of 43.6 °C and a minimum of 38.9 °C.

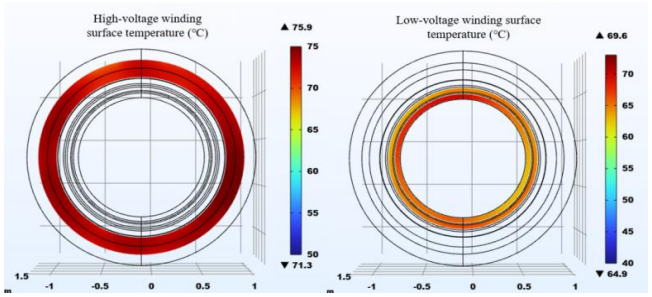

Fig. 5. Transformer winding arrangement and winding connections.

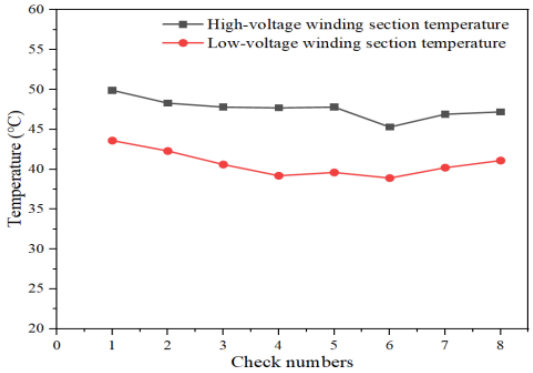

Fig. 6. Temperature distribution of the cut surface.

The temperature difference between the maximum and minimum points on the HV winding is 4.6 °C and that on the LV winding is 4.7 °C. These simulation results reveal discernible variations in the temperature distribution across individual disks of the transformer winding; however, the overall pattern conforms to an axisymmetric distribution within acceptable error limits. Therefore, it is feasible to substitute the 3D winding model with a 2D axisymmetric model for further analysis.

IV. TRANSFORMER TEMPERATURE RISE TESTS

A. Test Setup and Temperature Measurement Method

Authors wishing to include figures, tables, or text passages that have already been published elsewhere are required to obtain permission from the copyright owner(s) for both the print and online format and to include evidence that such permission has been granted when submitting their papers. Any material received without such evidence will be assumed to originate from the authors.

The experimental setup used a single-phase DPI-400000/500 dual-core column transformer operating at rated voltage. For temperature monitoring during the thermal rise test, a multichannel fluorescence-based fiber optic temperature measurement system was used [20], [21]. Six discrete temperature sensors were strategically positioned at the 3rd, 4th, and 5th disk segments of both the high-voltage and low-voltage windings, establishing six independent measurement channels. The precise installation details of the optical fibers are illustrated in Fig. 7(a). To ensure safe routing of the fibers from the transformer interior and effective isolation between the internal oil environment and the external atmosphere, a specialised feedthrough flange assembly was implemented. This design, depicted in Fig. 7(c), facilitates the connection between internal and external distributed optical fibers while maintaining a

hermetic seal at the transformer tank wall. The arrangement of all internal fiber optic temperature monitoring points is systematically summarised in Table III.

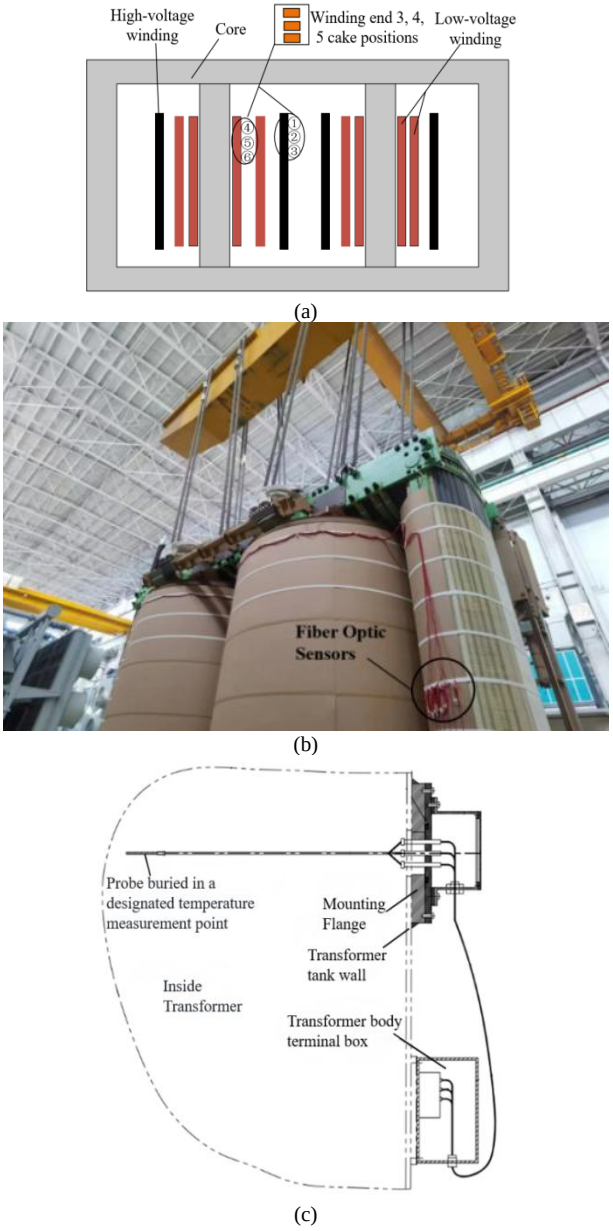

Fig. 7. Diagram of the fiber optic temperature measurement device: (a) Schematic of the fiber optic installation; (b) Field wiring of the fiber optic sensors; (c) Fiber optic temperature measurement connection diagram.

TABLE III. ARRANGEMENT OF THE FIBER OPTIC TEMPERATURE MEASUREMENT POINTS INSIDE THE TRANSFORMER.

Position	Name
High-voltage winding 3rd cake	Position 1
High-voltage winding 4th cake	Position 2
High-voltage winding 5th cake	Position 3
Low-voltage winding 3rd cake	Position 4
Low-voltage winding 4th cake	Position 5
Low-voltage winding 5th cake	Position 6

B. Results of Temperature Rise Tests

In the steady-state rated temperature test, the pressure is applied for approximately 13 hours, and when the temperature change of all temperature measurement points is less than 0.5 °C within one hour, the transformer operation reaches a stable state and the test is stopped. Figure 8 shows a histogram of the maximum temperature rise of the transformer's high-voltage windings and low-voltage windings measured by the optical fiber temperature measuring device when the transformer reaches the steady state. As illustrated in the figure below, the maximum temperature rises observed are 48.4 °C for the 5th disk of the high-voltage winding and 44.3 °C for the corresponding disk of the low-voltage winding. The corresponding experimental temperature rise data for both windings are comprehensively detailed in Table IV.

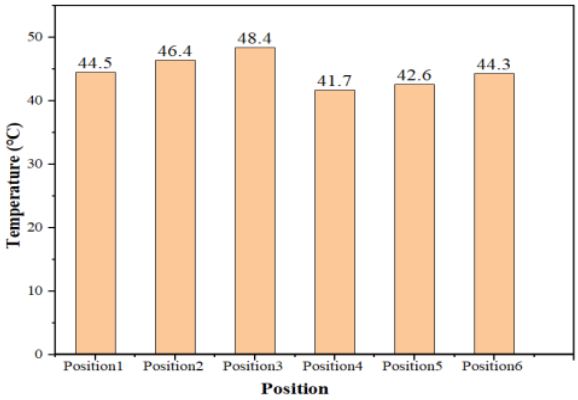

Fig. 8. Histogram of the temperature rise of the high-voltage and low-voltage windings.

TABLE IV. HIGH-VOLTAGE WINDING AND LOW-VOLTAGE WINDING TEST TEMPERATURE RISE.

	Cake 3rd temperature rise (°C)	Cake 4th temperature rise (°C)	Cake 5th temperature rise (°C)
High-voltage winding	44.5	46.4	48.4
Low-voltage winding	41.7	42.6	44.3

C. Analysis of Transformer Temperature Rise Test Results and Simulation Results

The results of the 3D simulation were compared with the temperature data of the fiber optic temperature measurement results. The 3D simulation temperature rise values are compared with the test temperature rise values, as shown in Fig. 9.

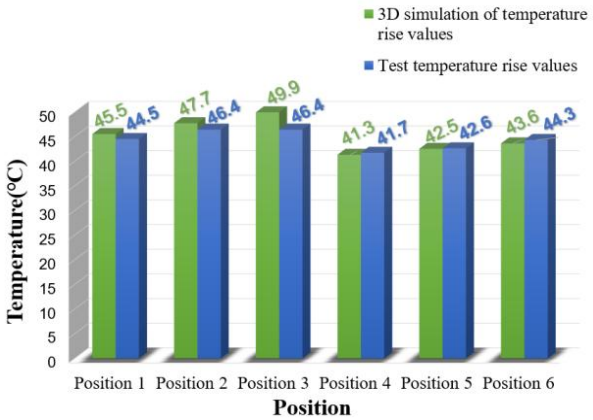

Fig. 9. Histogram of the 3D simulation temperature rise values and test temperature rise values.

The error results obtained are shown in Table V. As shown in Table V, the errors between the temperatures of the 3rd, 4th,

and 5th cakes of the high-voltage winding and the test value in the 3D simulation are 1 °C, 1.3 °C, and 1.5 °C, respectively. Moreover, the errors between the temperatures of the 3rd, 4th, and 5th cakes of the low-voltage winding and the test value are 0.4 °C, 0.1 °C, and 0.7 °C, respectively. The error rates are all within 3 %.

TABLE V. COMPARISON OF THE 3D SIMULATION AND TEST TEMPERATURE RISE VALUES.

	3D simulation temperature rise values (°C)	**Test temperature rise values (°C)**	**Error rates** (%)
Position 1	45.5	44.5	2.2
Position 2	47.7	46.4	2.8
Position 3	49.9	48.4	3.1
Position 4	41.3	41.7	0.96
Position 5	42.5	42.6	0.23
Position 6	43.6	44.3	1.6

According to the results of the 3D simulation of the transformer winding temperature distribution test results, the 3D simulation calculation of the transformer winding temperature distribution can accurately reflect the real transformer temperature rise state and can provide accurate data for the digital twin model of the transformer temperature field. However, due to the long 3D calculation time of approximately two hours and the large memory requirements, the temperature distribution of the transformer winding has good axisymmetric characteristics. Moreover, it is used to establish a 2D axisymmetric model of the winding and transformer oil instead of calculating a 3D simulation. Thus, the calculation time can be greatly shortened, and the real-time performance of the digital twin is improved to ensure accuracy.

V. 2D WINDING STRUCTURE OF SINGLE-PHASE TWO-CORE COLUMN NUCLEAR POWER MAIN TRANSFORMER

A. *Transformer 2D Winding Structure*

The 2D overall and local models of the windings in the transformer are shown in Fig. 10.

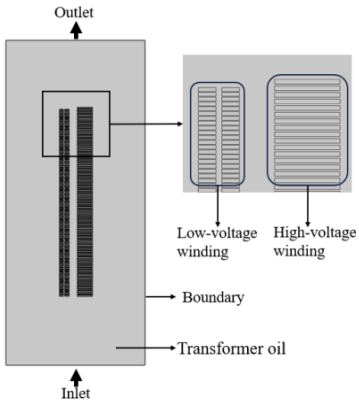

Fig. 10. Simulation results.

The model is mainly composed of the transformer oil and the winding, and the geometric dimensions are 1.8 m × 4.255 m. The high-voltage coil is divided into 124 cakes, and the low-voltage coil is divided into two layers. The purpose is to better dissipate heat, and each layer contains 168 cakes. The geometric model can better reflect the temperature distribution between the windings.

B. *Simulation Results*

This study focusses primarily on investigating the thermal performance of oil-immersed transformers. To accurately capture their actual temperature rise characteristics, the external ambient temperature was set at 26 °C, and the velocity at the oil flow inlet located on the underside of the transformer was specified as 0.05 m/s. Given that the simulation was conducted in two dimensions and considered only one side of the winding, the heat generation rate assigned to the winding in the 2D model was set to half of that used in the 3D simulation.

Figure 11 displays the temperature distribution across the windings and transformer oil under rated operating conditions. As observed, the high-voltage winding exhibits higher temperatures compared to the low-voltage winding. The thermal hotspot was identified within cakes 3 to 15 of the high-voltage winding. This phenomenon is attributed to the upward flow of transformer oil from the bottom, which removes a significant portion of the heat, resulting in lower temperatures in the lower half of the winding relative to the upper half.

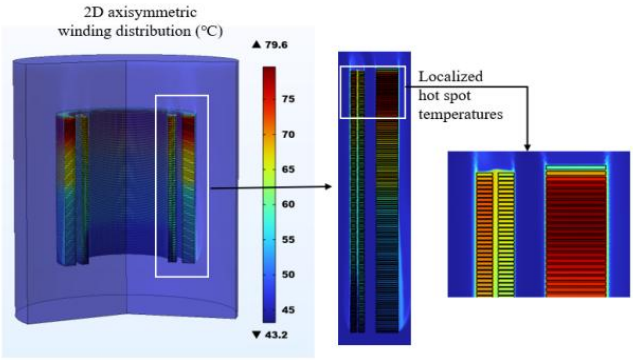

Fig. 11. Winding temperature distribution.

The calculated average temperature rises were 18.8 °C for transformer oil, 31.9 °C for low-voltage winding, and 35.2 °C for high-voltage winding. The maximum temperature rises reached 47.1 °C and 53.6 °C for the low-voltage and high-voltage windings, respectively.

A comparative analysis of the temperature rise values obtained from the 2D simulation, 3D simulation, and experimental tests is presented in the line charts of Fig. 12.

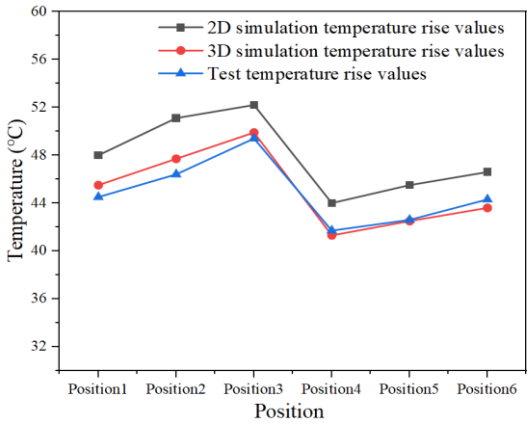

Fig. 12. Comparison of the temperature rise values obtained by different calculation methods.

The results indicate a discernible discrepancy between the 2D simulation outcomes and those of both the 3D model and the physical tests, with a maximum recorded error of 4.7 °C. Further comparison of error rate, detailed in Table VI, shows that the maximum deviation between the 2D simulated temperature rise and the values from the 3D simulation and experimental measurements was 10 %.

TABLE VI. COMPARISON OF THE 3D SIMULATION AND TEST TEMPERATURE RISE VALUES.

	2D simulation temperature rise value (℃)	**Error rate of temperature rise with 3D simulation (%)**	**Error rate of temperature rise with test (%)**
Position 1	48	5.5	7.9
Position 2	51.1	7.1	10.1
Position 3	52.2	4.6	7.9
Position 4	44	6.5	5.5
Position 5	45.5	7	6.8
Position 6	46.6	6.9	5.2

C. Adaptive Mesh-based Control Method of H-Type

From the above error data, it can be seen that the winding temperature error in the 2D simulation is relatively large. In response to the above, first, a better initial mesh is obtained through the free dissecting method. Second, the control method of the h-type adaptive mesh refinement is adopted. Finally, the computational accuracy is improved by subdividing the mesh regions with large errors in the initial mesh and then rerunning the finite element analysis so that the maximum size h of the local cells is reduced, avoiding the mesh redundancy caused by global encryption and improving the quality of mesh dissection during the calculation of the fluid-thermal coupling field of the main transformer of a single-phase two-core column nuclear power plant in a targeted manner. The schematic diagram of the local encryption of the grid is shown in Fig. 13, and the adaptive mesh optimisation of the transformer winding model is shown in Fig. 14.

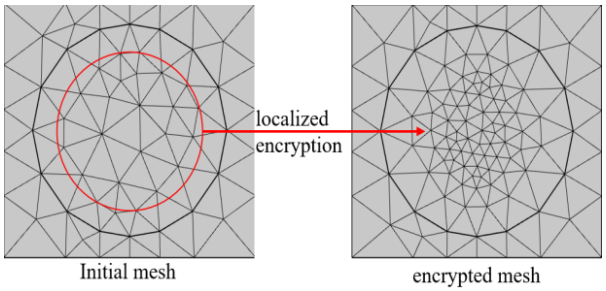

Fig. 13. Schematic diagram of localised encryption.

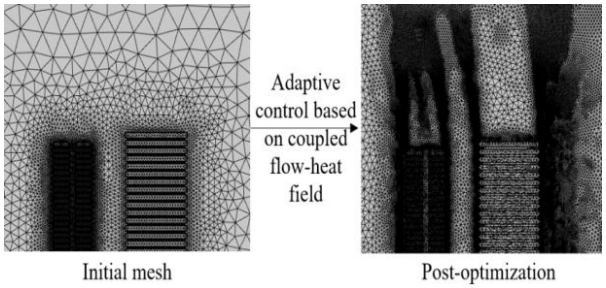

Fig. 14. Map of adaptive mesh control optimisation.

A two-dimensional axisymmetric simulation was performed using the optimised mesh configuration while maintaining all other initial boundary conditions unchanged. The resulting temperature distribution across the windings is illustrated in Fig. 15. The computed average temperature rises were 17.7 °C for the transformer oil, 30.7 °C for the low-voltage winding, and 32.7 °C for the high-voltage winding. The maximum temperature elevations reached 44.7 °C in the low-voltage winding and 50.2 °C in the high-voltage winding.

A comparative analysis of the maximum winding temperature rises obtained from 2D simulation, optimised 2D simulation, 3D simulation, and experimental testing is presented in Fig. 16. The results demonstrate that the maximum temperature rise derived from the model optimised via the h-type adaptive mesh refinement method shows strong agreement with both experimental measurements and 3D simulation values, confirming the feasibility of this approach.

Regarding computational efficiency, the 3D simulation required approximately two hours to complete, whereas the 2D simulation was accomplished in about 10 minutes, representing only 8 % of the 3D computation time. The 2D approach also required substantially less computational resources and memory capacity.

The error rates between the optimised 2D simulation, the 3D simulation, and the experimental hotspot temperature rise are summarised in Table VII. All observed discrepancies remained within 2.5 %, validating both the accuracy of the simulation optimisation and the capability of the refined 2D axisymmetric model to effectively represent the actual transformer winding temperature rise. Furthermore, when compared to the methodology described in [22], the h-type adaptive mesh refinement technique employed in this study yields a more precise temperature distribution of the transformer windings, exhibiting a lower error rate relative to the experimental data.

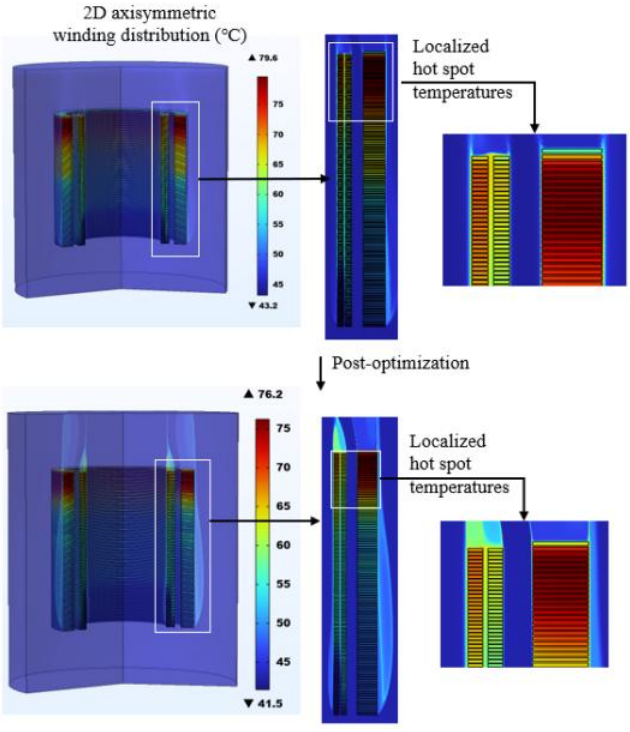

Fig. 15. Temperature distribution of the optimised winding.

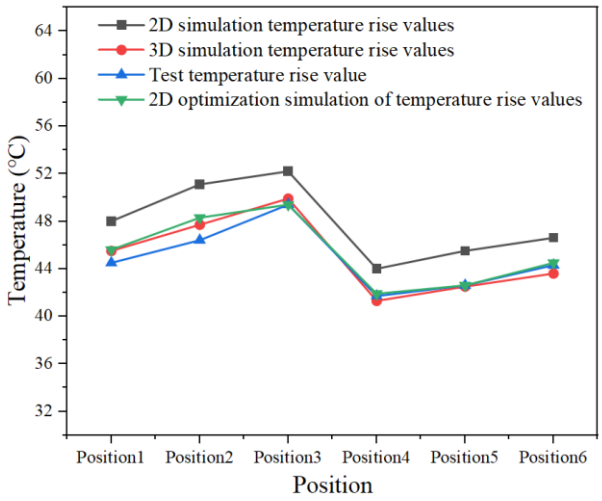

Fig. 16. Comparison of the temperature rise values obtained by different calculation methods.

TABLE VII. COMPARISON OF THE ERROR RATES OF DIFFERENT CALCULATION METHODS.

	2D Optimisation simulation of temperature rise value (°C)	Error rate of temperature rise with 3D simulation (%)	Error rate of temperature rise with test (%)
Position 1	45.6	0.22	2.5
Position 2	48.3	1.3	4.1
Position 3	49.4	1	2.1
Position 4	41.9	1.5	0.47
Position 5	42.6	0.24	0
Position 6	44.5	2.1	0.45

D. Distribution of the Winding Temperature under Different Load Conditions

Based on the optimised 2D axisymmetric model of the transformer rated operation, the eight loading conditions of 10 %, 30 %, 50 %, 70 %, 90 %, 110 %, 130 %, and 150 % of the rated load are simulated and calculated. Moreover, the results are compared with the 3D working condition simulation of the transformer. The comparison chart of the 2D and 3D condition simulations is shown in Fig. 17. As seen from the figure, the maximum values of the windings in the 2D axisymmetric and 3D simulation results of the transformer are basically the same, indicating that the use of 2D axisymmetric simulation instead of 3D simulation can ensure the accuracy of the temperature distribution data. Therefore, the optimised 2D axisymmetric model cannot only improve the calculation speed, but also ensure the accuracy of the calculated data. Additionally, it is more suitable for the construction of a transformer digital twin model than a 3D simulation model.

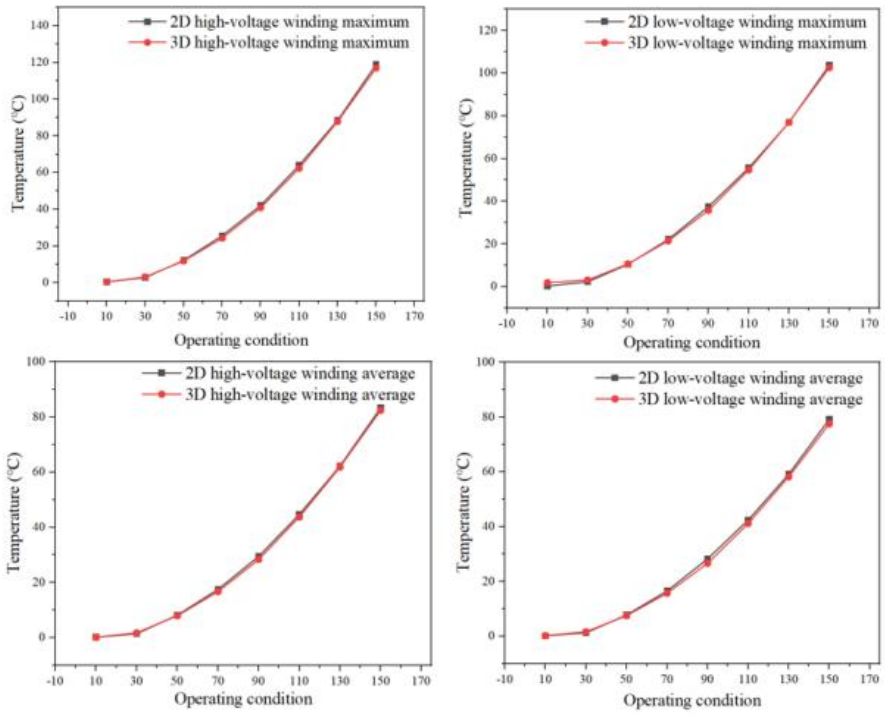

Fig. 17. Comparison of the 2D working condition simulation and the 3D working condition simulation.

E. Transformer Digital Twin Model Visualisation

On the basis of the preceding analysis, a comprehensive temperature database for the winding is constructed using simulation results derived from the two-dimensional optimised model across multiple working conditions. These data are subsequently mapped onto a three-dimensional digital twin platform of the winding, achieving a significant reduction in computational time while maintaining high result accuracy. The developed digital twin representation of the transformer is illustrated in Fig. 18. By adjusting the magnitude of the load current, the corresponding temperature distribution of the winding under various operational loads can be visualised in real time. This capability provides substantial support to operational and maintenance personnel, facilitating informed decision-making in management practices.

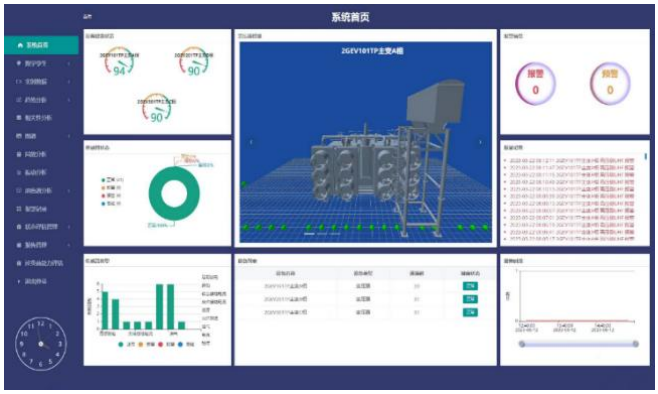

Fig. 18. 3D digital twin model of the transformer.

Figures 19–21 show the winding temperature distribution under 50 %, 100 %, and 150 % of the rated load.

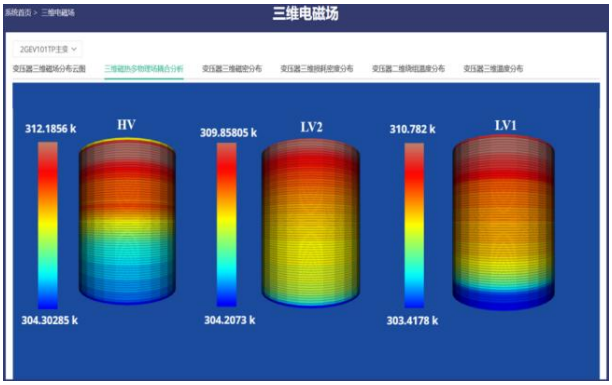

Fig. 19. Temperature distribution of the 50 % windings of the rated load.

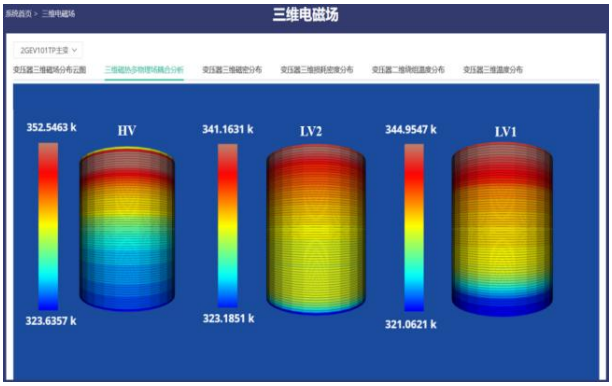

Fig. 20. Temperature distribution of the rated load windings.

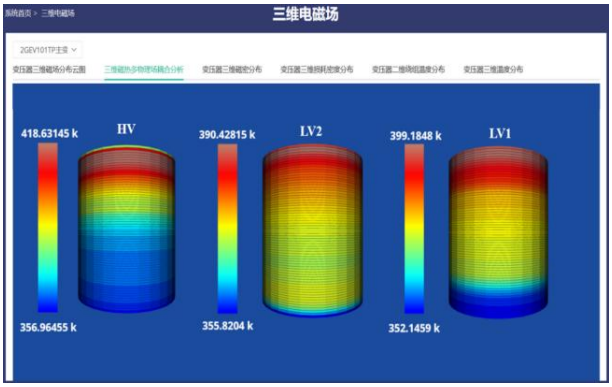

Fig. 21. Temperature distribution of the 150 % windings of the rated load.

It can be seen from the figure that the temperature distribution diagram of the windings of the 3D digital twin model is basically consistent with the temperature distribution of the 3D simulated model. However, the 3D simulation time is about two hours, while the 3D digital twin model simulation time is about five seconds, which is about 0.069 % of the 3D simulation time, and the simulation time is greatly reduced.

A comparative analysis was conducted between the winding temperature rise values derived from the 3D digital twin model of the transformer under 50 %, 100 %, and 150 % of the rated load conditions and those obtained from the 3D simulation. The results of this comparison are presented in Fig. 22. As illustrated, the discrepancy in winding temperature between the 3D digital twin and the 3D simulation remains minimal across various loading scenarios, with all observed errors confined within a 3 °C margin.

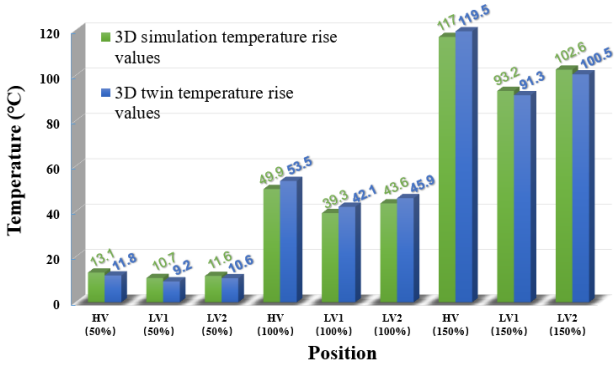

Fig. 22. Comparison of 3D digital twin models and 3D simulation models under different working conditions.

Furthermore, the winding temperature rise from the 3D digital twin model at rated load was validated against experimental measurements, with the comparative data detailed in Table VIII. The analysis reveals that the error rate between the digital twin predictions and the empirical data is within 8.8 %, which falls within an acceptable engineering tolerance.

TABLE VIII. COMPARISON OF 3D TWIN VALUES WITH TEST VALUES.

	3D twin temperature rise values (℃)	**Test temperature rise values** (℃)	**Error rate from the test temperature rise value** (%)
Position 1	44.6	44.5	0.2
Position 2	48.1	46.4	3.7
Position 3	51.1	48.4	8.8
Position 4	42.7	41.7	2.3
Position 5	44.7	42.6	4.9
Position 6	45.4	44.3	2.5

These comparisons with high-fidelity simulation and physical testing confirm the accuracy and reliability of the developed 3D digital twin model, demonstrating its substantive value for practical engineering applications. A direct visual comparison of the temperature rise values from the digital twin and the experimental measurements is provided in Fig. 23.

VI. CONCLUSIONS

In this paper, a 500 kV single-phase two-core column

nuclear power main transformer is simulated and studied on fluid-thermal coupling. Combined with the transformer temperature rise test, the correctness of the simulation analysis method is verified and the following conclusions are obtained.

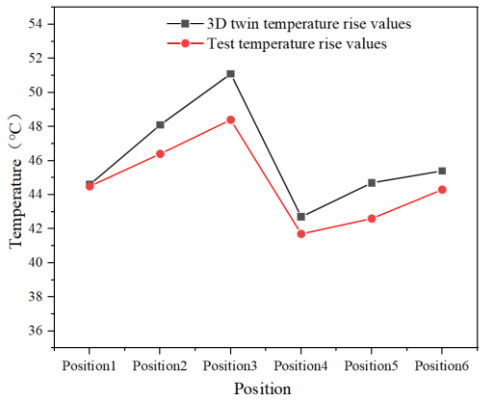

Fig. 23. Comparison of 3D twin values with test values.

1. To prevent the risks of local temperature increases, large leakage magnetic fields, and large short-circuit forces of single-column transformer windings, a single-phase two-core column nuclear power main transformer is adopted, whose special physical structure plays an obvious role in reducing magnetic leakage and controlling the local winding temperature overheating, saves costs to a certain extent, and reduces the occupation of space, which greatly reduces the risk of accidents.
2. Based on the h-type adaptive mesh control method, the mesh optimisation of a single-phase two-core column nuclear power main transformer is carried out to obtain the 2D optimisation simulation model of the transformer. By comparing the temperature rise of the corresponding part of the windings obtained from the fiber-optic temperature measurement test and the 3D simulation, the error rate of the temperature rise of the windings is within 4 %, which verifies the accuracy of the 2D optimisation simulation results.
3. The adoption of an optimised two-dimensional simulation model offers a substantial reduction in computational time compared to conventional three-dimensional modelling approaches, requiring only 8 % of the time required for equivalent 3D simulations. This improvement in efficiency enhances the feasibility of employing high-fidelity simulations in practical engineering applications. Furthermore, this method enables the comprehensive calculation of winding temperature distributions across diverse loading scenarios. The resulting dataset provides a valuable foundation for the construction of digital twin transformer models, thereby supporting operational and maintenance management and facilitating data-driven decision-making for personnel.

CONFLICTS OF INTEREST

The authors declare that they have no conflicts of interest.

REFERENCES

[1] Y. Jing, X. Wang, Z. Yu, C. Wang, Z. Liu, and Y. Li, "Diagnostic research for the failure of electrical transformer winding based on digital twin technology", *IEEJ Transactions on Electrical and Electronic Engineering*, vol. 17, no. 11, pp. 1629–1636, 2022. DOI: 10.1002/tee.23670.

[2] Z. Zhang and L. Lv, "Application status and prospects of digital twin technology in distribution grid", *Energy Reports*, vol. 8, pp. 14170–14182, 2022. DOI: 10.1016/j.egyr.2022.10.410.

[3] G. A. Diaz, E. E. Mombello, J. J. Perez, and D. F. Pinzon, "New method for fast coupled magnetic field-circuit simulation of power transformers based on a semi-analytical approach", *International Journal of Electrical Power & Energy Systems*, vol. 131, art. 106976, 2021. DOI: 10.1016/j.ijepes.2021.106976.

[4] T. Wu, F. Yang, U. Farooq, J. Jiang, and X. Hu, "Real-time calculation method of transformer winding temperature field based on sparse sensor placement", *Case Studies in Thermal Engineering*, vol. 47, art. 103090, 2023. DOI: 10.1016/j.csite.2023.103090.

[5] H. Yao *et al.*, "Simulation study on oil pressure problems caused by internal faults in oil-immersed transformers", *Process Safety and Environmental Protection*, vol. 175, pp. 190–198, 2023. DOI: 10.1016/j.psep.2023.05.053.

[6] K. Li, J. Li, Q. Huang, and Y. Chen, "Data augmentation for fault diagnosis of oil-immersed power transformer", *Energy Reports*, vol. 9, no. S10, pp. 1211–1219, 2023. DOI: 10.1016/j.egyr.2023.05.110.

[7] G. Kaliappan and M. Rengaraj, "Aging assessment of transformer solid insulation: A review", *Materials Today: Proceedings*, vol. 47, no. P1, 272–277, 2021. DOI: 10.1016/j.matpr.2021.04.301.

[8] R. Liao, S. Liang, C. Sun, L. Yang, and H. Sun, "A comparative study of thermal aging of transformer insulation paper impregnated in natural ester and in mineral oil", *European Transactions on Electrical Power*, vol. 20, pp. 518–533, 2009. DOI: 10.1002/etep.336.

[9] M. Nazmunnahar, S. Simizu, P. R. Ohodnicki, S. Bhattacharya, and M. E. McHenry, "Finite-element analysis modeling of high-frequency single-phase transformers enabled by metal amorphous nanocomposites and calculation of leakage inductance for different winding topologies", *IEEE Transactions on Magnetics*, vol. 55, no. 7, pp. 1–11, 2019. DOI: 10.1109/TMAG.2019.2904007.

[10] Z. Jurković, B. Jurišić, and T. Župan, "Multi-step approach for fast calculation of magnetic field in power transformer yoke shunt", *Electric Power Systems Research*, vol. 221, art. 109407, 2023. DOI: 10.1016/j.epsr.2023.109407.

[11] P. Pijarski, "Modelling of multi-winding transformers for short-circuit calculations in the power system – Modelling accuracy and differences in equivalent circuits", *International Journal of Electrical Power & Energy Systems*, vol. 148, art. 108971, 2023. DOI: 10.1016/j.ijepes.2023.108971.

[12] A. Kumar, B. R. Bhalja, and G. B. Kumbhar, "Novel technique for location identification and estimation of extent of turn-to-turn fault in transformer winding", *IEEE Transactions on Industrial Electronics*, vol. 70, no. 7, pp. 7382–7392, 2023. DOI: 10.1109/TIE.2022.3201309.

[13] L. Wang, X. Dong, L. Jing, T. Li, H. Zhao, and B. Zhang, "Research on digital twin modeling method of transformer temperature field based on POD", *Energy Reports*, vol. 9, no. S2, pp. 299–307, 2023. DOI: 10.1016/j.egyr.2023.03.010.

[14] J. Smolka, "CFD-based 3-D optimization of the mutual coil configuration for the effective cooling of an electrical transformer", *Applied Thermal Engineering*, vol. 50, no. 1, pp. 124–133, 2013. DOI: 10.1016/j.applthermaleng.2012.06.012.

[15] L. Raeisian, H. Niazmand, E. Ebrahimnia-Bajestan, and P. Werle, "Thermal management of a distribution transformer: An optimization study of the cooling system using CFD and response surface methodology", *International Journal of Electrical Power & Energy Systems*, vol. 104, pp. 443–455, 2019. DOI: 10.1016/j.ijepes.2018.07.043.

[16] N. A. Muhamad, H. Kamarden, and N. A. Othman, "Heat distribution pattern of oil-filled transformer at different hottest spot temperature locations", in *Proc. of 2015 IEEE 11th International Conference on the Properties and Applications of Dielectric Materials (ICPADM)*, 2015, pp. 979–982. DOI: 10.1109/ICPADM.2015.7295438.

[17] J. Li, Z. Liang, and S. Xu, "Research on modeling and grid connection stability of large-scale cluster energy storage power station based on digital mirroring", *Energy Reports*, vol. 8, no. S5, pp. 584–596, 2022. DOI: 10.1016/j.egyr.2022.02.234.

[18] D. Herrero-Pérez, S. G. Picó-Vicente, and H. Martínez-Barberá, "Efficient distributed approach for density-based topology optimization using coarsening and h-refinement", *Computers & Structures*, vol. 265, art. 106770, 2022. DOI: 10.1016/j.compstruc.2022.106770.

[19] X. Jia, M. Lin, S. Su, Q. Wang, and J. Yang, "Numerical study on temperature rise and mechanical properties of winding in oil-immersed transformer", *Energy*, vol. 239, part A, art. 121788, 2022. DOI: 10.1016/j.energy.2021.121788.

[20] M. Novkovic, A. Popovic, E. Briosso, R. Martinez Iglesias, and Z.

Radakovic, "Dynamic thermal model of liquid-immersed shell-type transformers", *International Journal of Electrical Power & Energy Systems*, vol. 142, part B, art. 108347, 2022. DOI: 10.1016/j.ijepes.2022.108347.

[21] A. Abdali, A. Abedi, H. Masoumkhani, K. Mazlumi, A. Rabiee, and J. M. Guerrero, "Magnetic-thermal analysis of distribution transformer: Validation via optical fiber sensors and thermography", *International Journal of Electrical Power & Energy Systems*, vol. 153, art. 109346, 2023. DOI: 10.1016/j.ijepes.2023.109346.

[22] N. Ling, X. Du, W. An, J. Wu, X. Li, and S. Li, "Temperature field simulation analysis of distribution transformers based on fluid-temperature field coupling", in *Proc. of 2023 International Conference on Power Energy Systems and Applications (ICoPESA)*, 2023, pp. 896–900. DOI: 10.1109/ICoPESA56898.2023.10141040.